Evolution of the Potential-Energy Surface of Amorphous Silicon

Houssem Kallel,* Normand Mousseau,† and François Schiettekatte‡

Département de Physique and Regroupement Québécois sur les Matériaux de Pointe (RQMP), Université de Montréal, C.P. 6128, Succursale Centre-Ville, Montr éal, Québec, Canada H3C 3J7

(Received 19 April 2010; published 22 July 2010)

The link between the energy surface of bulk systems and their dynamical properties is generally difficult to establish. Using the activation-relaxation technique, we follow the change in the barrier distribution of a model of amorphous silicon as a function of the degree of global relaxation. We find that while the barrier-height distribution, calculated from the initial minimum, is a unique function that depends only on the level of relaxation, the reverse-barrier height distribution, calculated from the final state, is independent of global relaxation, following a different function. Moreover, the resulting gained or released energy distribution is a simple convolution of these two distributions indicating that the activation and relaxation parts of the elementary relaxation mechanism are completely independent. This characterized energy landscape can be used to explain nanocalorimetry measurements.

DOI: 10.1103/PhysRevLett.105.045503 PACS numbers: 61.43.Dq, 61.43.Bn, 65.60.+a, 66.30.−h

The concept of energy landscape has been used extensively in the last decade to characterize the properties of complex materials. In finite systems, such as clusters and proteins, the classification of energy minima and energy barriers has shown that it is possible to understand, using single-dimension representations such as the disconnectivity graph, the fundamental origin of cluster dynamics and protein folding [1]. Because of the explosion in the number of barriers in bulk systems, these analyses have been mostly limited there to the characterization of the overall structure of the energy landscape through the disconnectivity graph or the inherent structure method [1]. While these approaches have been very fruitful, many questions remain regarding the evolution of the local structure of the energy landscape itself as a function of global relaxation, an evolution that determines the dynamics of disordered materials away from equilibrium [2].

The approach followed here leaves aside the global features of the energy landscape captured by these methods and focuses rather directly on its detailed structure around specific minima at a different degree of relaxation. This extensive local sampling allows us to extract energy-barrier distributions and to understand the dynamics of disordered materials away from equilibrium. More precisely, we focus on amorphous silicon (*a*-Si), a model system studied extensively, both experimentally and theoretically, over the years [2–4]. Using the activation-relaxation technique (ART nouveau) [5], a saddle-point finding method, we characterize the evolution of the local energy landscape, defined by the distribution of transition states and adjacent energy minima around a local configuration, as a function of global relaxation, i.e., overall energy decrease. The resulting theoretical picture can be used to understand and explain recent nanocalorimetric measurements on ion-implanted *a*-Si samples [2,6]. As we will show, results presented here tie experiments and simulations and provide a clear link between the structure of the energy landscape and experimental observations, supporting the importance of this concept.

Our *a*-Si model is relaxed using the Stillinger-Weber potential with parameters adjusted specifically to recover the structural and vibrational properties of the amorphous system [7]. While this potential has a number of shortcomings, its structural evolution as a function of relaxation is in good qualitative agreement with experiment as discussed below. Moreover, it is fast enough to allow for an extensive search of transition states, necessary to construct reliable energy distributions. Starting from a 4000-atom random configuration in a cubic box with periodic-boundary conditions, the system is relaxed using ART nouveau: beginning in a local energy minimum, the system is brought to an adjacent transition state and relaxed into a new minimum. The move is accepted using a Metropolis criterion with a temperature of 0.25 eV, following Refs. [4,5]. A total of 95 445 events is necessary to relax the model from an initial energy per atom of -2.89 eV/atom going down to -3.04 eV/atom (see Fig. 1 in inset). Figure 1 shows the correlation between the energy per atom and the bond-defect concentration (mostly threefold and fivefold coordinated Si). Following this global relaxation, we find a linear relation between the width of the transverse optic (TO) peak, calculated using the relation of Ref. [8], and the configurational energy, with a slope of 0.989 (kJ/mol)/deg, in good agreement with experiment [6,9].

To characterize the evolution of the local energy landscape as a function of the degree of global relaxation, we explore extensively the transition state distributions around four configurations with decreasing internal stress. The energy per atom for these configurations is indicated in Table I. From each of these four generic configurations, we generate 100 000 events (exit pathways), providing a detailed picture of the local energy landscape associated with various degrees of relaxation. In each case, we remove the

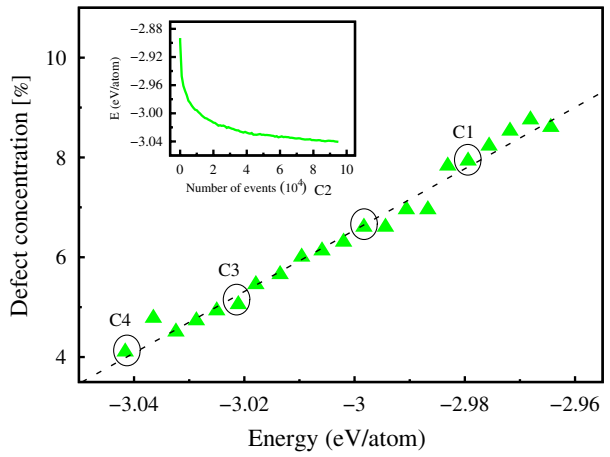

FIG. 1 (color online). Fraction of coordination defects (mostly threefold and fivefold coordinated atoms) as a function of the configurational energy per atom (in eV) for the 4000-atom model of *a*-Si. The large circles indicate the location of the four configurations selected for further analysis. Inset: energy per atom as a function of event during the preparation of the configurations.

duplicate events leaving about 12 000 different activated pathways from the initial local minimum to a nearby one for each of these four configurations, i.e., about 12 000 different transition points and adjacent minima. The nature of dominant activated mechanisms in *a*-Si have already been discussed elsewhere [4,10,11] and we focus here on the distribution of forward and reverse barrier heights (measured, respectively, from the transition state to the initial and final state) and energy asymmetry (given by the energy difference between the final and initial state), for each level of global relaxation. From previous analysis, we know that although the total number of events in *a*-Si is between 30 and 60 per atom, the overall distribution converges relatively quickly [4] and we observe only negligible differences in the shape of the various energy distributions by including the events generated after 50 000 or 100 000 ART moves.

From transition state theory, we know that the kinetics of activation-dominated systems is controlled by the rate of escape from the initial energy minimum. Figure 2(a) shows the distribution of activation barriers from the initial minimum to the transition state (forward barrier or FB) for configurations *C*1 to *C*4. We observe that the distribution is continuous and bounded in agreement with previous simulations [4,10] but also that it shifts towards higher energy as the configurations are relaxed. As shown in Fig. 3(a), however, the four curves are well represented by the same function given by a Gaussian multiplied by the energy:

$$G_{\mathrm{FB}}(E) = AE \exp\left\{-\frac{(E - \langle E_{\mathrm{FB}}^{\mathrm{rel}}\rangle)^2}{2\sigma_{\mathrm{FB}}^2}\right\} \qquad (1)$$

where, as is shown in Table I, the peak position controlled by $E_{\mathrm{FB}}^{\mathrm{rel}}$ varies with the degree of global relaxation but the overall scale A and the width of the distribution, given by σ_{FB}, are constant. Remarkably, the shift in $E_{\mathrm{FB}}^{\mathrm{rel}}$ is significantly larger than the drop in the average strain per atom as the configuration is relaxed: $E_{\mathrm{FB}}^{\mathrm{rel}}$ shifts by 0.67 eV from *C*1 to *C*4 as the energy per atom decreases by only 0.06 eV. This result is consistent with the growing super-Arrhenius relaxation time scale observed in strong glasses and generally described by the empirically-derived Vogel-Fulcher law [12]. However, while this relation postulates a constant energy barrier and an unusual temperature relation, we see here that the reverse is happening: it is the barrier height that increases with relaxation. The disproportionate shift in

TABLE I. Properties of the four sampled 4000-atom *a*-Si configurations including energy per atom and the fitting parameters to Eq. (1) for the forward-barrier (FB) distribution

	*C*1	*C*2	*C*3	*C*4
Energy/atom	−2.980	−2.996	−3.019	−3.042
$\langle E_{\mathrm{FB}}\rangle$ (eV)	1.919	2.190	2.430	2.587
σ_{FB} (eV)	1.178	1.153	1.141	1.164
A (eV^{-2})	0.17	0.16	0.14	0.13

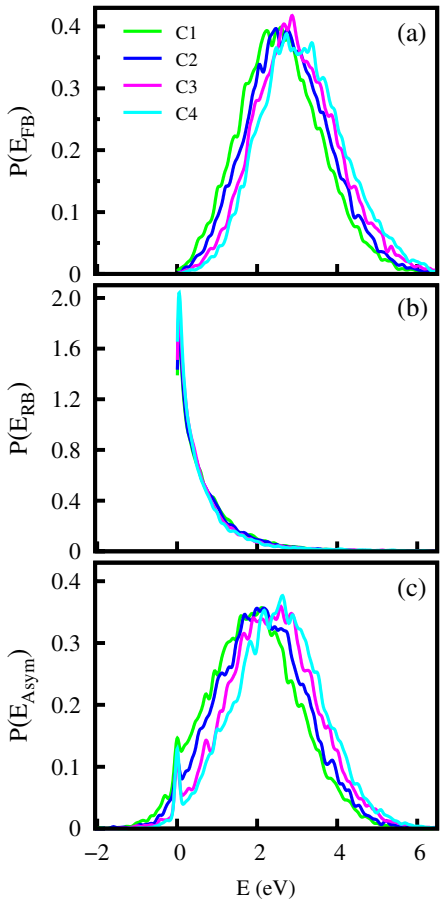

FIG. 2 (color online). (a) Forward and (b) reverse energy-barrier distribution, and (c) asymmetry energy distribution for configurations *C*1 to *C*4.

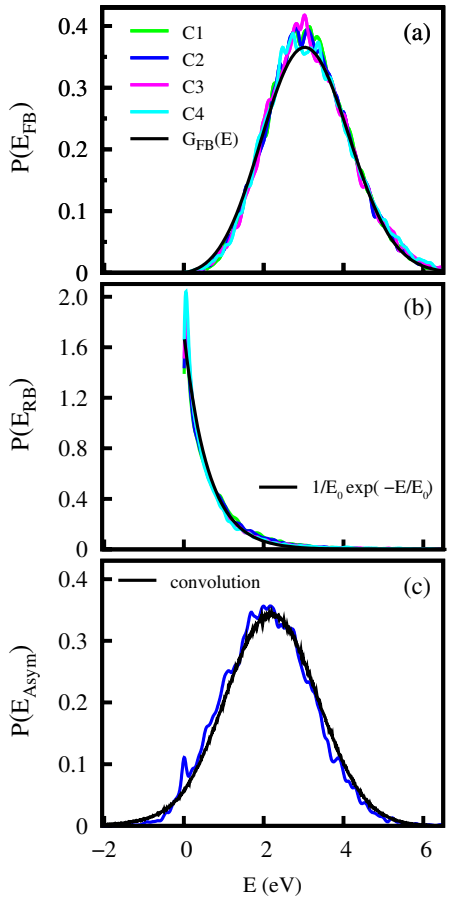

FIG. 3 (color online). Collapsed (a) forward and (b) reverse energy-barrier distributions, following the equations given in the text. (c) Asymmetry distribution for configuration $C2$ and the corresponding distribution generated by convoluting the respective forward and reverse-barrier distributions.

the forward-barrier distribution as a function of relaxation can be explained by previous observations that the defected and strained local environments play a major role in the evolution of amorphous systems as diffusion or rearrangement in perfectly coordinated regions of the amorphous network tend to have an energy cost similar to that of the crystal [3,10].

Even though a system's kinetics is conditioned by the barrier height between minima, the long time evolution of a system is also determined by the overall event energy asymmetry. For example, if a system jumps onto a very energetic state, with a high-energy asymmetry with respect to the initial minimum, it will come back immediately onto the initial state irrespective of the height of the forward energy barrier. In effect the presence of these highly asymmetric states surrounding a local minimum only slows down the relaxation. To characterize this phenomenon, we plot the reverse energy-barrier distribution [Fig. 2(b)], i.e., the energy-barrier height measured from the final minimum. As had been observed before, we note that the forward and reverse energy-barrier distributions are qualitatively different [4]: instead of a Gaussian, we observe an exponential distribution with a large proportion of irrelevant states and very few low-energy minima contributing to the evolution of a-Si into a more stable local state (also observed for Lennard-Jones and a-Si in a slightly different setup in Ref. [4,13]). Contrary to the behavior of the forward-energy distribution, we find that the reverse energy-barrier distribution is essentially independent of the global relaxation level, with the exception of regions of very low-energy, zero eV where the identification of recurring events is sometimes tricky. Neglecting this region, we see that all backward barrier distributions are represented by the same exponential, $\exp(-\Delta E/E_0)$, where $E_0 = 0.60$ eV [see Fig. 3(b)].

These two distributions, forward and backward, cannot be measured directly experimentally. However, the heat released during relaxation is directly associated with the energy asymmetry, i.e., the energy difference between the initial and final minima. Figure 2(c) shows the energy asymmetry distribution surrounding configurations $C1$ to $C4$, a structure that changes with the degree of relaxation. While the shape of the distribution looks complex, it is a simple convolution of the two independent forward and backward energy-barrier distributions, as is shown in Fig. 3(c). Not only do these two distributions behave differently with the relaxation, these turn out to be independent: the height of a barrier does not provide any information regarding the energy of the final minimum. While this result seems to contradict the Bell-Evans-Polanyi principle [14], a numerical analysis of catastrophe theory shows that these correlations hold only for very short pathways [15].

The energy landscape picture developed here can be used to explain recent differential nanocalorimetric measurements made on implanted a-Si [2,6], offering an experimental check on these results. Samples are implanted at low temperature and then heated, while heat released is measured, revealing a number of features: First, the heat flux released as the sample is heated is relatively uniform as a function of temperature, for temperatures ranging from 118 to 775 K; second, the stored strain, measured as the heat rate, saturates as a function of implantation fluence; third, for low fluences, the heat-rate follows nearly the same curve, irrespective of the implantation temperature. For fluences near saturation, the heat release amplitude increases with decreasing implantation temperature. These results were explained by the presence of a continuous distribution of states where each annealing event releases an amount of heat independent of its activation energy. Dynamic annealing was considered responsible for the increasing signal with decreasing temperature near saturation: some configurations are only accessible if underlying, low activation energy configurations survived dynamic annealing.

The saturation of stored strain can be readily explained within the context of energy landscape: We have seen that the barrier-height distribution shifts to lower energy as the strain level increases. As this shifts occurs, the number of barriers within $k_B T$ increases reaching a point, for a given

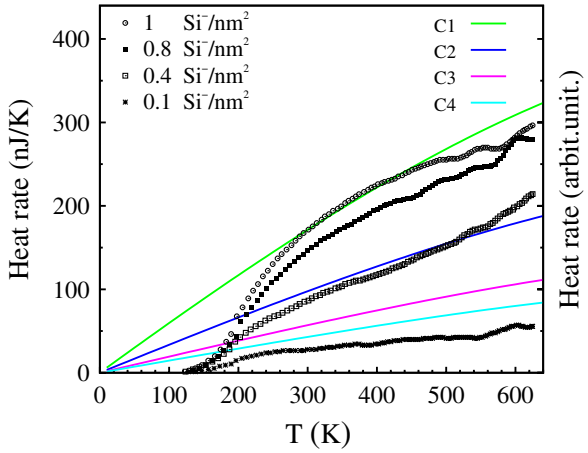

FIG. 4 (color online). Heat flux as a function of temperature for Configurations $C1$ to $C4$ (lines) compared with the heat flux released during relaxation of ion-implanted a-Si samples (experimental data from Karmouch *et al.* [2]).

temperature, at which relaxation takes place faster than the strain increase, leading to the saturation.

Understanding the behavior of the released heat-flux requires more analysis. For this, we suppose that since the energy-barrier distribution shifts rapidly to higher energy as the system is relaxed, low-energy barriers present in the initial configuration, before heating is started, are not replaced: once a barrier is ''used'' it does not reappear at once because heating is relaxing the system. We do not have to worry about the change in shape at high energy because these events have an exponentially small probability of occurring during the fast heating. Because the reverse distribution is independent of the global relaxation state, we also pose that it remains constant during the heating process. Although a precise quantitative comparison is difficult to do, considering that the size of the ion-implanted region is about 10^{16} atoms with a heating rate of 30 kK/s, an attempt frequency of 10^{13} s^{-1} and about 50 events per atom [4], we obtain for $C1$ at 600 K a heat release of about 10^{-7} J/K, in line with the experiment.

Starting from one initial minimum, we assign a temperature-dependent Boltzmann probability of crossing each barrier, posing a constant attempt frequency [11]. Using a constant heating rate, we select forward-energy barriers with the Bolztmann-weighted probability times the probability distribution and the reverse barrier with the exponential distribution. An event is accepted only if the final state has an energy lower than the initial state, since high-energy states will be unstable and will jump back immediately to the original minimum. The resulting heat flux, shown in Fig. 4, compares very well with the experimental results allowing us to relate this behavior to two factors: first, the number of barriers being crossed as a function of temperature increases linearly only (because T is very small with respect to E_{FB}) and most barriers crossed are of the order of a few k_BT. However, since most of the weight in the reverse-barrier distribution is concentrated near zero, the number of crossings actually releasing heat does not change significantly, leading to the experimentally observed uniform increase as a function of temperature. We can see in Fig. 4, moreover, that the number of heat releasing events decreases significantly at low fluence due to the exponential form of the reverse-barrier distribution.

In conclusion, the extensive sampling of the energy landscape of a-Si allows us to extract energy-barrier distributions that, surprisingly, follow well-defined but different analytical expressions for the forward and backward energy barriers. These distributions, moreover, are totally independent from each other, contrary to what could have been expected [14], but with the same end result. These results, that reproduce and explain recent nanocalorimetry measurement of heat released after ion implantation, provide microscopic information complementary to more large scale energy landscape studies [1,16]. While it remains to be confirmed numerically, the picture developed here should apply to covalent glasses in general.

This work was funded in part by the Canada Research Chairs program, the Fonds québécois de recherche sur la nature et les technologies (FQRNT) and NSERC. Calculations were done using resources from the Réseau Québecois de Calcul de Haute Performance (RQCHP). H. K. is grateful to the Tunisian Government for financial support.

*houssem.kallel@umontreal.ca
†normand.mousseau@umontreal.ca
‡francois.schiettekatte@umontreal.ca

[1] David J. Wales, *Energy Landscapes. Applications to Clusters, Biomolecules and Glasses* (Cambridge Molecular science, Cambridge, 2004).
[2] R. Karmouch *et al.*, Phys. Rev. B **75**, 075304 (2007).
[3] D. A. Drabold, Eur. Phys. J. B **68**, 1 (2009).
[4] F. Valiquette and N. Mousseau, Phys. Rev. B **68**, 125209 (2003).
[5] R. Malek and N. Mousseau, Phys. Rev. E **62**, 7723 (2000).
[6] J.-F. Mercure, R. Karmouch, Y. Anahory, S. Roorda, and F. Schiettekatte, Phys. Rev. B **71**, 134205 (2005).
[7] R. L. C. Vink *et al.*, J. Non-Cryst. Solids **282**, 248 (2001).
[8] R. L. C. Vink, G. T. Barkema, and W. F. van der Weg, Phys. Rev. B **63**, 115210 (2001).
[9] S. Roorda *et al.*, Phys. Rev. B **44**, 3702 (1991).
[10] G. T. Barkema and N. Mousseau, Phys. Rev. Lett. **81**, 1865 (1998).
[11] Y. Song, R. Malek, and N. Mousseau, Phys. Rev. B **62**, 15680 (2000).
[12] H. Vogel, Z. Phys. **22**, 645 (1921); G. S. Fulcher, J. Am. Ceram. Soc. **8**, 339 (1925).
[13] T. F. Middleton and D. J. Wales, Phys. Rev. B **64**, 024205 (2001).
[14] K. A. Dill and S. Bromberg, *Molecular Driving Forces* (Garland Science, New York, 2008).
[15] D. J. Wales, Science **293**, 2067 (2001).
[16] A. Heuer, J. Phys. Condens. Matter **20**, 373101 (2008).